

Supporting Information for

Encapsulating $[\text{Mo}_3\text{S}_{13}]^{2-}$ clusters in cationic covalent organic framework: Enhancing stability and recyclability by conversion from homogeneous to heterogeneous photocatalyst

Yuan-Jie Cheng,^{‡ab} Rui Wang,^{‡a} Shan Wang,^a Xiao-Juan Xi,^a Lu-Fang Ma^{*ab} and Shuang-Quan Zang^{*a}

^a College of Chemistry and Molecular Engineering, Zhengzhou University, Zhengzhou 450001, China.

^b College of Chemistry and Chemical Engineering, Henan Key Laboratory of Function-Oriented Porous Materials, Luoyang Normal University, Luoyang 471934, China

E-mail: zangsqzg@zzu.edu.cn

E-mail: mazhuxp@126.com

Experimental Details

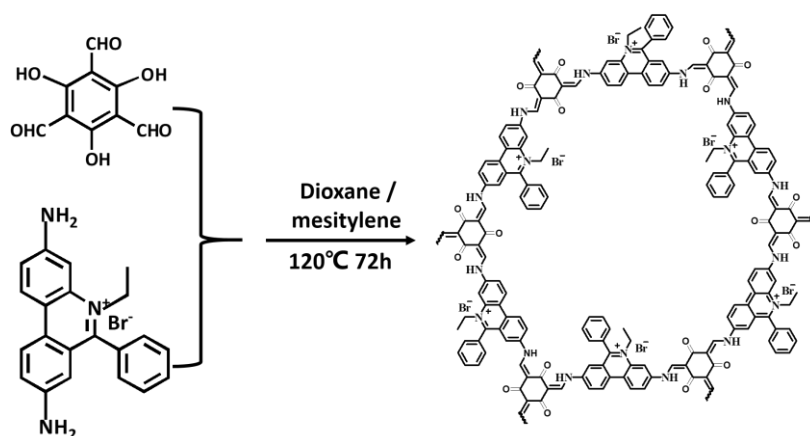
All chemicals were of reagent grade quality and gained from commercial sources. Powder X-ray powder diffraction (PXRD) patterns were recorded by using a PANalytical EMPYREAN diffractometer with Cu K α 1 radiation ($\lambda = 1.540598 \text{ \AA}$) at room temperature. Diffraction intensity data for 2θ from $2.5\text{-}60^\circ$ were collected at the scanning speed of 1 sec/step with 2θ step increment of 0.0131° . ^1H NMR spectra were recorded on a Bruker DRX spectrometer operating at 400 MHz in CDCl_3 . ^{13}C MAS solid-state NMR experiments were performed on Agilent 600 DD2 spectrometer at a resonance frequency of 150.15 MHz. ^{13}C NMR spectra were recorded with spinning rate of 15kHz with a 4mm probe at room temperature. ^{13}C CPMAS experiments were performed with a delay time of 5s. Scan number: 2048 scans. X-ray photoelectron spectroscopy (XPS) were recorded with EscaLab 250Xi. Atomic Force Microscope (AFM) were recorded with NT-MDT Prima. Inductively coupled plasma mass spectrometry (ICP-MS) were recorded with OptiMass 9500/NMR-213. The photoluminescence (PL) emission spectra were recorded with HORIBA FluoroLog-3 spectrofluorometer. Nitrogen sorption isotherms were measured at liquid nitrogen temperature (77 K) by using automatic volumetric adsorption equipment (Belsorp Max) after a degassed process at 100°C for 12 h. Specific surface areas were obtained by using the Brunauer-Emmet-Teller (BET) model, pore size distributions were simulated by the nonlocal density functional theory (NLDFT) model, and the pore volumes were calculated from the amount adsorbed at $P/P_0=0.99$. FT-IR spectra were measured on a Nexus 870 FTIR spectrometer from KBr pellets as the sample matrix. Elemental analysis was performed on a scanning electron microscopy (SEM) measurement was carried out using Zeiss Sigma 500. UV-Vis diffuse reflectance spectra (DRS) were measured with a TU-1901 double-beam UV-Vis spectrophotometer.

Synthesis of 1, 3, 5-triformylphloroglucinol (Tp)

Tp was synthesized according to the procedures described in the literatures.^{1,2} To Hexamethylenetetramine (15.098 g, 108 mmol) and 1,3,5-Trihydroxybenzene (6.014

g, 49 mmol) under N₂ was added 90 mL trifluoroacetic acid. The solution was heated to 100 °C and maintained for ca. 2.5 h. With addition of 150 mL of 3 M HCl, the mixture was kept at 100 °C for another 1 h. After cooling to room temperature, the solution was filtered, extracted with dichloromethane (4 × 100 mL), dried over anhydrous Mg₂SO₄, and filtered. Rotary evaporation of the solvent afforded the orange powder. The solid was repeatedly washed with hot ethanol to get a light pink powder (1.28 g, yield: 22%). ¹H NMR (400 MHz, CDCl₃): δ (ppm) 14.16 (s, 3H, OH), 10.19 (s, 3H, CHO).

Synthesis of EB-COF

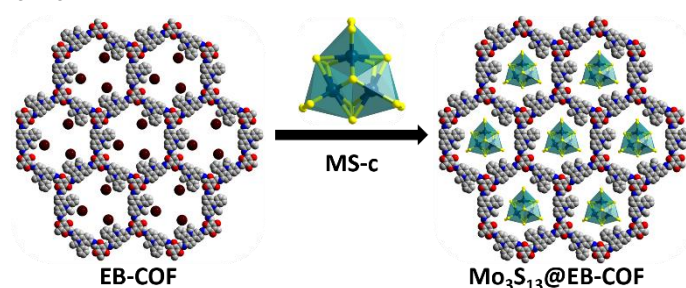


EB-COF was synthesized according to the procedures described in the literatures.³ A Pyrex tube (10×8 mm² and length 18 cm) is charged with Tp (0.1 mmol, 21 mg), ethidium bromide (EB) (0.15 mmol, 59 mg), 2 mL 1,4-dioxane-mesitylene (v/v, 1:1), 0.2 mL of 6M aqueous acetic acid. The tube was then flash frozen at 77 K (liquid N₂ bath) and degassed by three freeze-pump-thaw cycles. The tube was sealed off and then heated at 120 °C for 3 days. After that we turn off the oven and the cooling process is implementing undisturbed. A dark red precipitate was collected by filtration and washed with THF thrice. The powder collected was then solvent exchanged with THF and Methanol and dried at 100 °C under vacuum for 12 hours to get EB-COF (60 mg, yield: ~ 85%).

Synthesis of MS-c

The MS-c was synthesized according to the procedures described in the literatures.⁴ 4.0 g of $(\text{NH}_4)_6\text{Mo}_7\text{O}_{24} \cdot 4\text{H}_2\text{O}$ was dissolved in 20 ml water in an Erlenmeyer flask. An ammonium polysulfide solution (120 ml, 25 wt.%) was added and the flask was covered with a watch glass. The solution was then kept on an oil bath at 96 °C for five days without stirring. Dark-red powders of MS-c precipitated and were removed by filtering, followed by washing successively with water and ethanol. To remove excess sulphur, the MS-c were heated in hot toluene at ~ 80 °C for 2-4 hours. Finally, the powders were dried in air (5.3 g, yield: ~ 90%).

Synthesis of $\text{Mo}_3\text{S}_{13}@EB\text{-COF}$



MS-c (150 mg) was dissolved in 0.05 mol/L NaHCO_3 solution (250 mL) in a 500 mL vessel. Then 100 mg EB-COF was added and stirred at room temperature for 24 hours. After that, the mixed solution was centrifuged and washed with deionized water until the filtrate was colourless. Repeated the above step and the precipitate was dried in vacuum gave $\text{Mo}_3\text{S}_{13}@EB\text{-COF}$ (110 mg, yield: ~ 73%).

Synthesis of MIL-100(Fe)

The MIL-100(Fe) was synthesized according to the procedures described in the literatures, but with some important modifications.⁵ 56 mg Fe powder, 150 mg benzene tricarboxylic (1,3,5-BTC), 0.4 mL HF, 0.6 mL 1 mol/L HNO_3 , 5 mL H_2O that was held at 160 °C in a Teflon-lined autoclave for 12 hours. The light-orange solid product was recovered by filtration and washed with deionized water. A treatment was performed sequentially in hot deionised water (80 °C) for 3 hours, in ethanol (60 °C) for 3 hours, in 38 mmol/L NH_4F solution (70 °C) for 3 hours. A light-orange solid was collected by filtration, and dried at 80 °C under vacuum for 12 hours.

Synthesis of Mo₃S₁₃@MIL-100(Fe)

MS-c (113 mg) was dissolved in methanol (250 mL) in a 500 mL vessel. Then 135 mg MIL-100(Fe) was added in and stirred at room temperature for 24 hours. After that, the mixed solution was centrifuged, washed with methanol and deionized water until colourless. Repeated the above step and the precipitate was dried in vacuum, giving Mo₃S₁₃@MIL-100(Fe) (106 mg, yield: ~ 78%).

Photocatalytic hydrogen evolution of Mo₃S₁₃@EB-COF

The photocatalytic hydrogen production experiments and conditions optimization experiments were performed in a 50 mL quartz cell using a 300 W Xe lamp (PLS-SXE300C produced by Beijing Perfect Light Technology Co. Ltd) equipped with a UV cut off filter ($\lambda > 420$ nm). The experiments were performed in a mixture solution of DMF/H₂O which dissolved the photosensitizer and sacrificial reagent, and suspended with catalyst powder following ultrasonic dispersion for 20 min. Prior to irradiation, the system was deaerated by bubbling nitrogen for 15 min. During the photocatalytic reaction, the reactor was tightly sealed to avoid gas exchange and maintained at 25 °C. The generated hydrogen in the headspace was sampled (300 μ L) and then analyzed using gas chromatography (Agilent Technology 7820A, nitrogen as a carrier gas) equipped with a thermal conductivity detector (TCD).

For long-time hydrogen evolution experiments, 0.5 mg of Mo₃S₁₃@EB-COF dispersed in 15 mL of 1:1 DMF/H₂O solvent together with 300 mM/L of ascorbic acid (abbreviated as L-Vc) as the sacrificial electron donor and 10 mg Ru(bpy)₃Cl₂ (abbreviated as Ru(bpy)₃) as photosensitizer.

For photocatalyst cycle experiments, two reaction systems were prepared. System A: 6 mg of Mo₃S₁₃@EB-COF dispersed in 15 mL of 1:1 DMF/H₂O solvent together with 50 mM/L of L-Vc and 10 mg Ru(bpy)₃, the system A was photocatalyst cycle experiment; System B: 24 mg of Mo₃S₁₃@EB-COF dispersed in 60 mL of 1:1 DMF/H₂O solvent together with 50 mM/L of L-Vc as the sacrificial electron donor

and 40 mg Ru(bpy)₃ as photosensitizer. System B is used as catalysts in system A to recover the necessary loss of replenishment. For each cycle the photocatalyst (Mo₃S₁₃@EB-COF) was separated from its suspension (for the photocatalytic measurements) by centrifugation and was washed several times with water. The dried photocatalyst was redispersed with a fresh photocatalytic reaction solution (The photocatalytic cycle reaction dose according to system A; the photocatalytic replenishment response dose control system A is expanded, such as system B) and illuminated for 5 hours ($\lambda > 420$ nm) for each cycle.

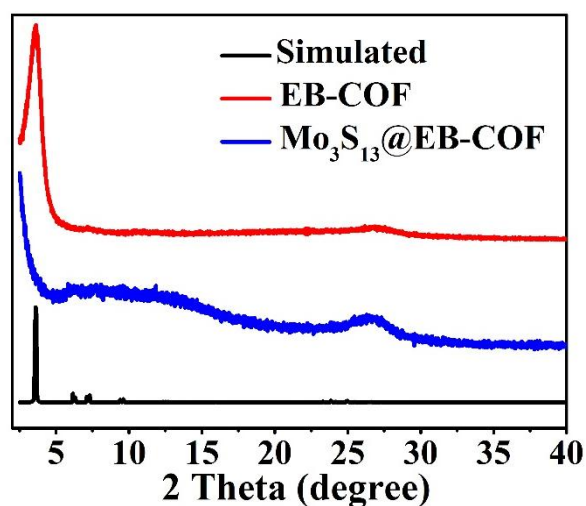


Figure S1. PXRD patterns of EB-COF and Mo₃S₁₃@EB-COF.

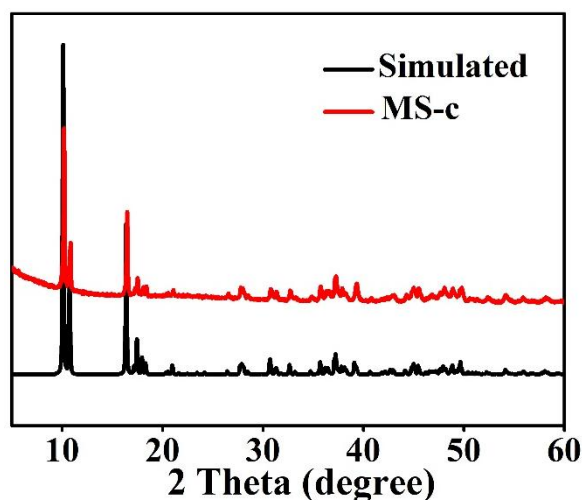


Figure S2. PXRD patterns of synthesized and simulated MS-c.



Figure S3. The filtrate of MS-c in different solvents.



Figure S4. The filtrate of Mo_3S_{13} @EB-COF in different solvents after 24 hours soakage.

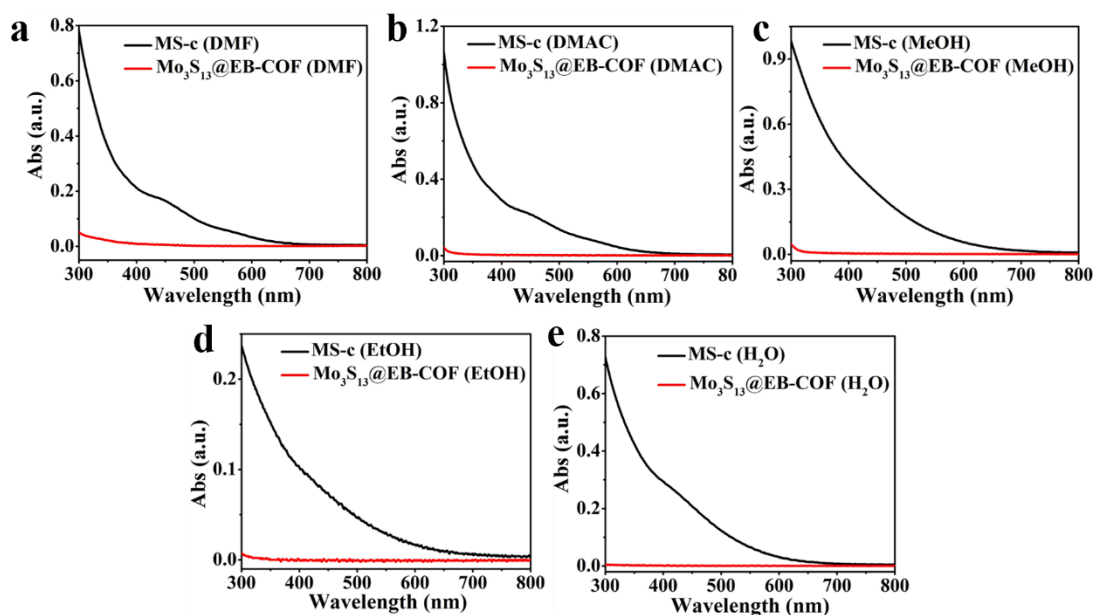


Figure S5. Liquid-phase UV-vis spectra from leaching test of $\text{Mo}_3\text{S}_{13}@EB\text{-COF}$ in DMF (a); DMAC (b); MeOH (c); EtOH (d); H_2O (e).

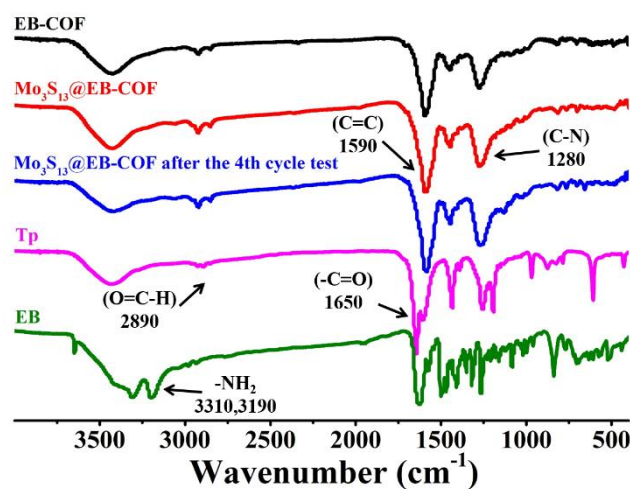


Figure S6. FT-IR spectra of EB-COF, $\text{Mo}_3\text{S}_{13}@EB\text{-COF}$, $\text{Mo}_3\text{S}_{13}@EB\text{-COF}$ after the 4th cycle test, Tp, and EB. The co-condensation reaction through the disappearance of characteristic absorption peaks of the N-H stretching bands of EB ($3190, 3310\text{ cm}^{-1}$) and the aldehyde group stretching bands of Tp ($\text{C}=\text{O}$ at 1650 cm^{-1} , $\text{O}=\text{C}-\text{H}$ at 2890 cm^{-1}) prove to be accomplished. EB-COF and $\text{Mo}_3\text{S}_{13}@EB\text{-COF}$ have a same characteristic peak ($\text{C}=\text{C}$ at 1590 cm^{-1}).

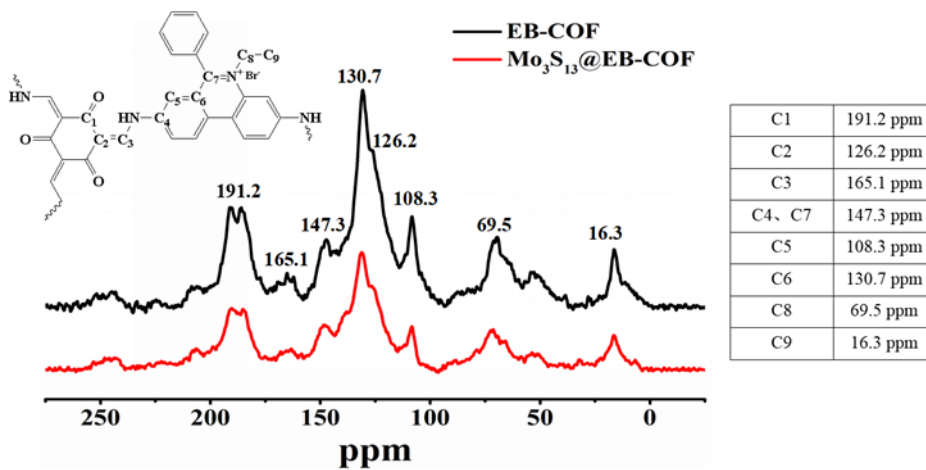


Figure S7. ^{13}C CP-MAS solid-state NMR spectra EB-COF and Mo_3S_{13} @EB-COF.

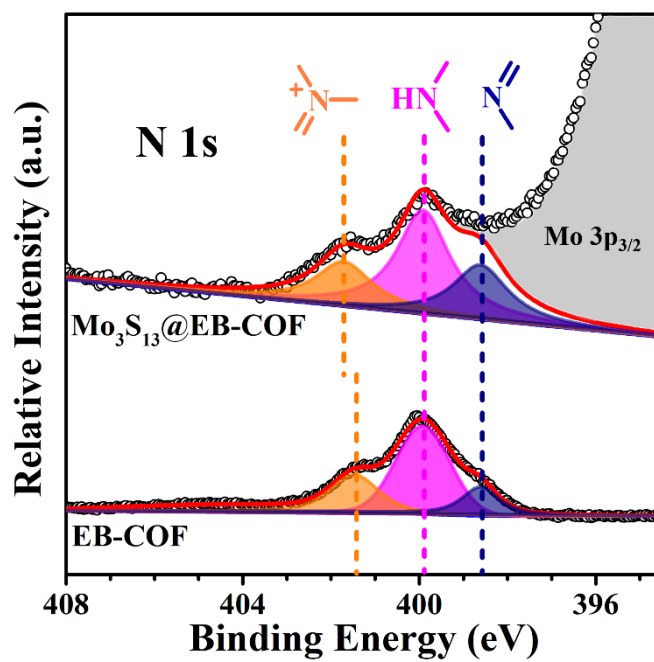


Figure S8. XPS spectra of N 1s for EB-COF and Mo_3S_{13} @EB-COF.

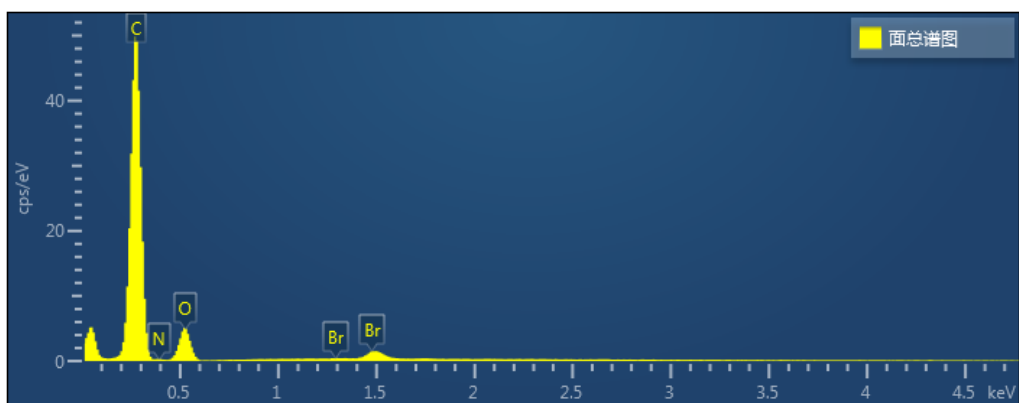


Figure S9. EDS elemental analysis of EB-COF.

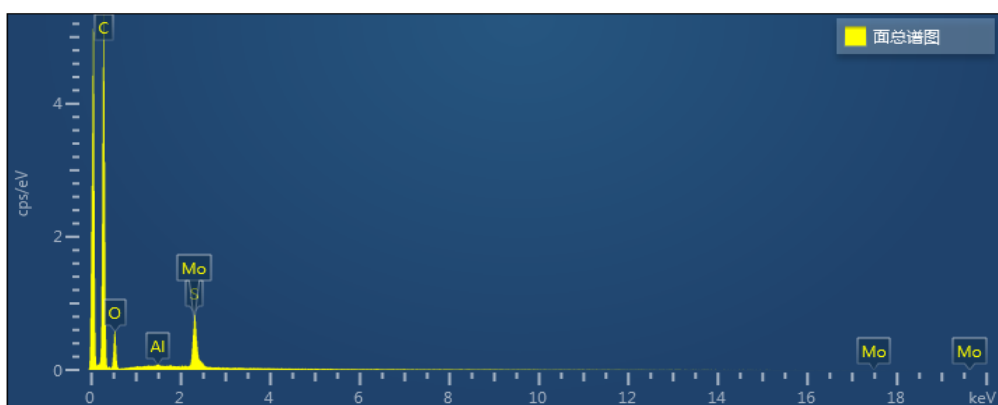


Figure S10. EDS elemental analysis of Mo_3S_{13} @EB-COF.

Table S1: The C, H, N and S elemental analysis of EB-COF and Mo_3S_{13} @EB-COF.

	C[%]	N[%]	H[%]	S[%]
theoretical value of EB-COF	60.68	7.86	4.02	0.00
EB-COF	60.28	7.64	4.07	0.00
theoretical value of completely exchanged Br ⁻ ions with bivalent $[\text{Mo}_3\text{S}_{13}]^{2-}$ anions in Mo_3S_{13} @EB-COF	40.19	5.21	2.67	25.83
Mo_3S_{13} @EB-COF	33.80	4.42	2.36	25.22

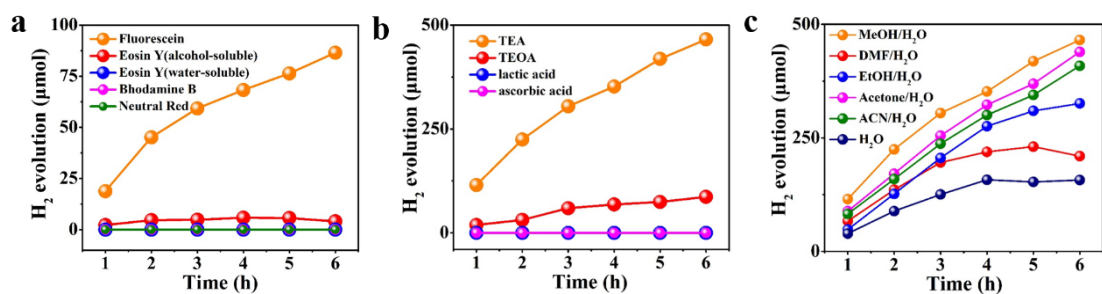


Figure S11. The effect of the photosensitizer (a), sacrificial agent (b) and solvent (c) on H₂ evolution of MS-c.

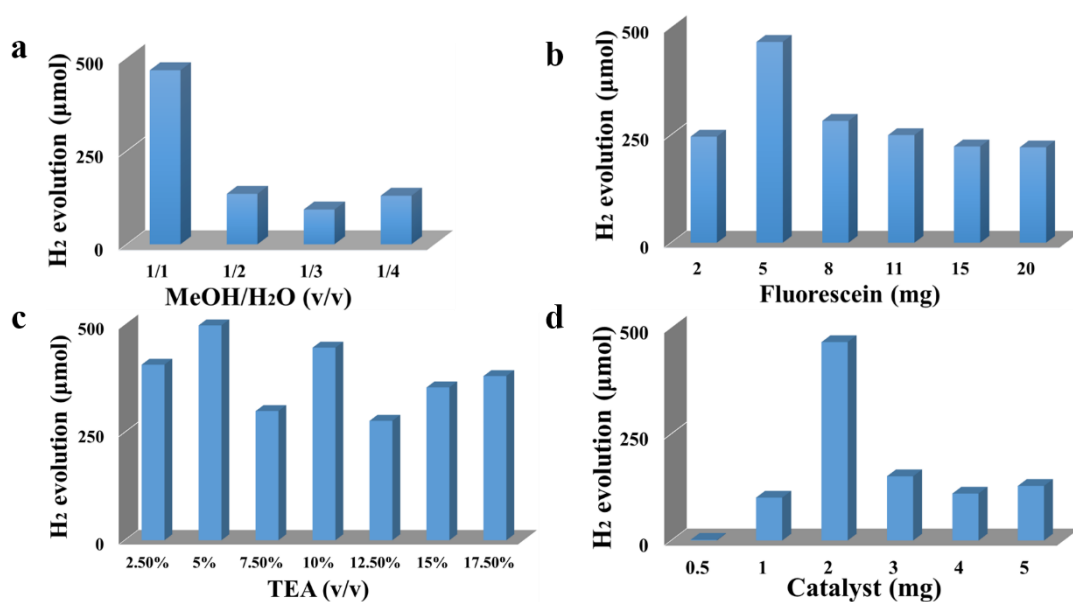


Figure S12. The effect of the volume ratio of MeOH/H₂O (a), the amount of fluorescein (b), the volume ratio of TEA (c), the amount of catalyst (d) on H₂ evolution of MS-c.

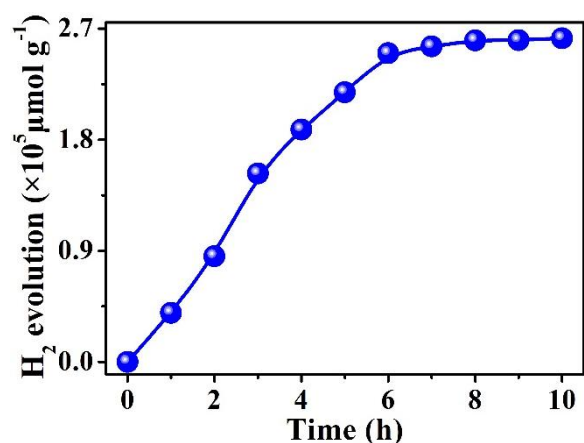


Figure S13. Time course of hydrogen evolution from MeOH/H₂O (1:1) 20mL solution with 2 mL TEA; 5 mg fluorescein and 2 mg MS-c under visible light irradiation over 10 hours.

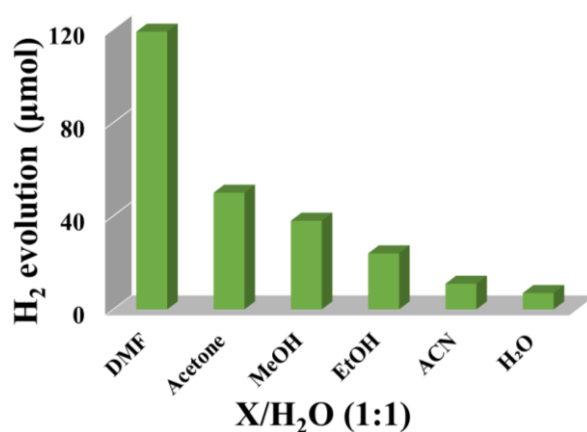


Figure S14. The effect of the solvent on H₂ evolution, H₂ evolution condition: DMF/H₂O (1:1), Acetone/H₂O (1:1), MeOH/H₂O (1:1), EtOH/H₂O (1:1), ACN/H₂O (1:1), and pure water in the presence of 2 mg of Mo₃S₁₃@EB-COF in 15 mL solution containing 50 mmol/L of L-Vc and 10 mg Ru(bpy)₃ under a nitrogen atmosphere. The system was irradiated with a 300 W Xe lamp with a cutoff filter of 420 nm for 6 hours.

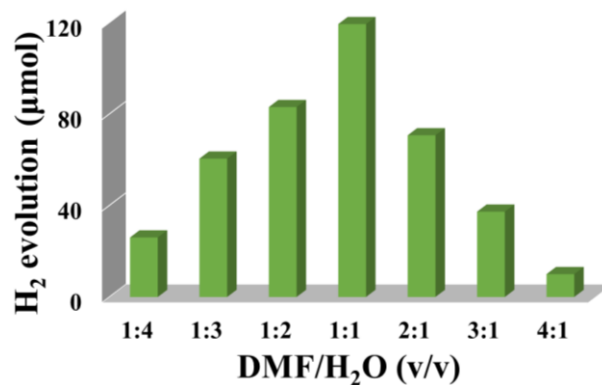


Figure S15. The effect of the volume ratio of DMF/H₂O on photocatalytic H₂ evolution in the presence of 2 mg of Mo₃S₁₃@EB-COF in 15 mL solution containing 50 mmol/L of L-Vc and 10 mg Ru(bpy)₃ under a nitrogen atmosphere. The system was irradiated with a 300 W Xe lamp with a cutoff filter of 420 nm for 6 hours.

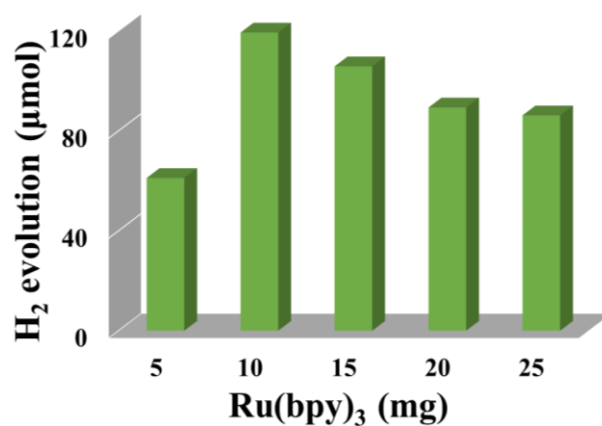


Figure S16. The effect of the quantity of photosensitizer on H₂ evolution, H₂ evolution condition: DMF/H₂O (1:1) in the presence of 2 mg of Mo₃S₁₃@EB-COF in 15 mL solution containing 50 mmol/L of L-Vc and the different quantity of Ru(bpy)₃ under a nitrogen atmosphere. The system was irradiated with a 300 W Xe lamp with a cutoff filter of 420 nm for 6 hours.

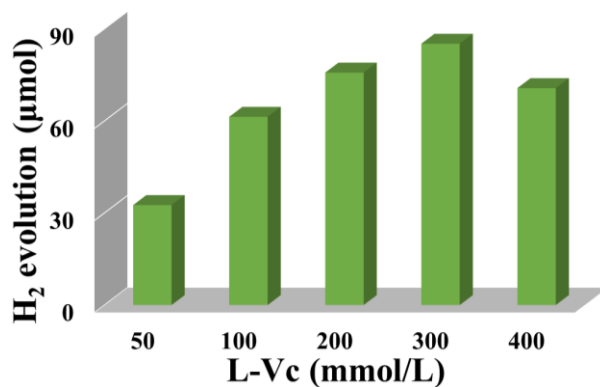


Figure S17. The effect of the concentration of the sacrificial electron donor on H₂ evolution, H₂ evolution condition: DMF/H₂O (1:1) in the presence of 2 mg of Mo₃S₁₃@EB-COF in 15 mL solution containing the different concentrations of L-Vc and 10mg Ru(bpy)₃ under a nitrogen atmosphere. The system was irradiated with a 300 W Xe lamp with a cutoff filter of 420 nm for 6 hours.

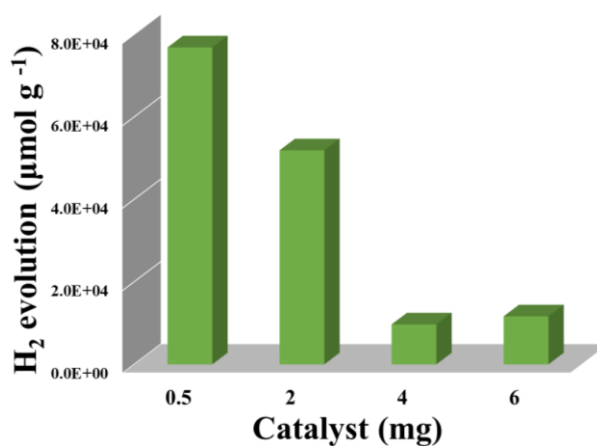


Figure S18. The effect of the quality of catalyst on H₂ evolution, H₂ evolution condition: DMF/H₂O (1:1) in the different quality of Mo₃S₁₃@EB-COF in 15 mL solution containing 300 mmol/L of L-Vc and 10 mg of Ru(bpy)₃ under a nitrogen atmosphere. The system was irradiated with a 300 W Xe lamp with a cutoff filter of 420 nm for 6 hours.

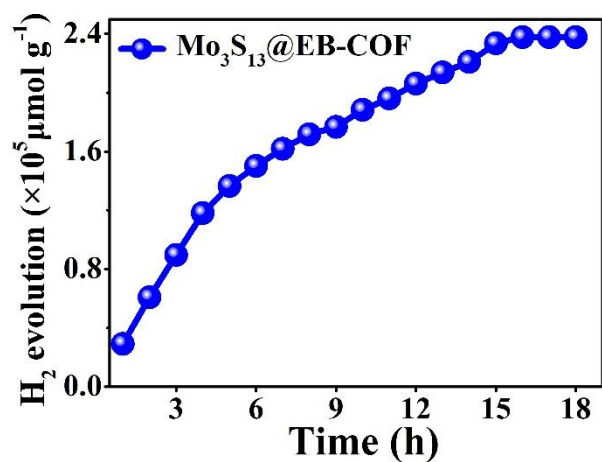


Figure S19. Time course of hydrogen evolution from DMF/H₂O (1:1) 15mL solution with 300 mmol/L L-Vc; 10 mg Ru(bpy)₃ and 0.5 mg Mo₃S₁₃@EB-COF. The system was irradiated with a 300 W Xe lamp with a cutoff filter of 420 nm for 18 hours.



Figure S20. EDS elemental analysis of the filtrate after photocatalytic hydrogen evolution.

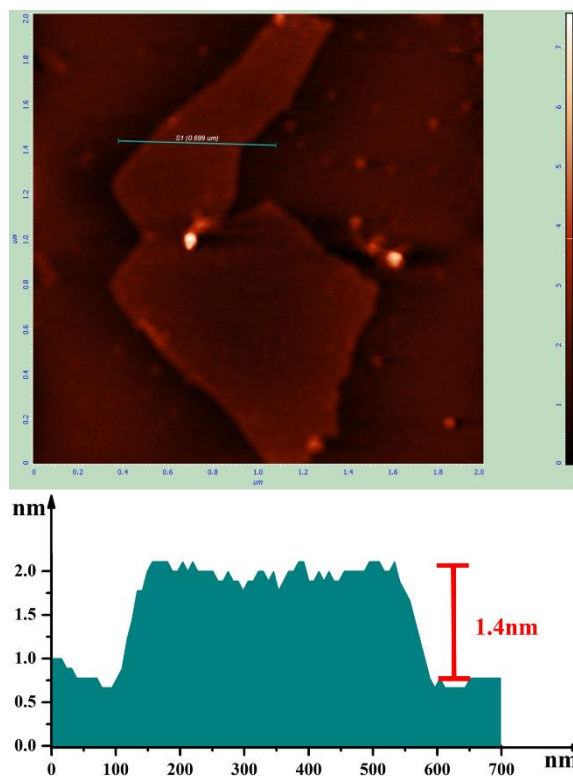


Figure S21. AFM image and height profile of Mo₃S₁₃@EB-COF.

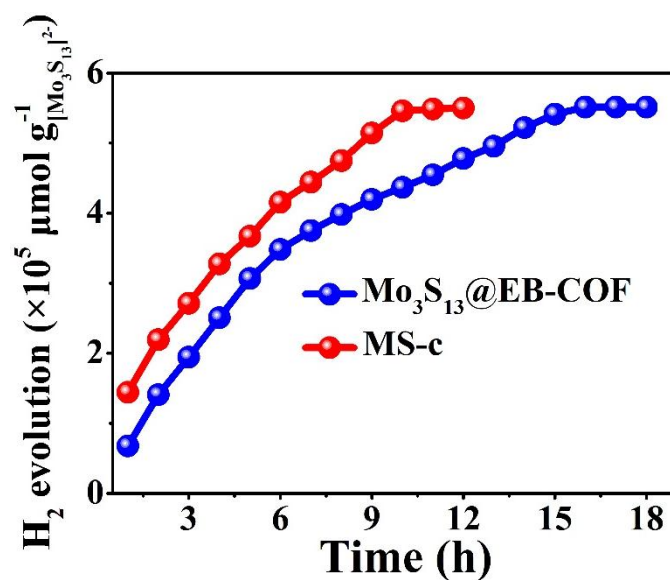


Figure S22. Hydrogen evolution of MS-c and Mo₃S₁₃@EB-COF based on same mass of the [Mo₃S₁₃]²⁻.

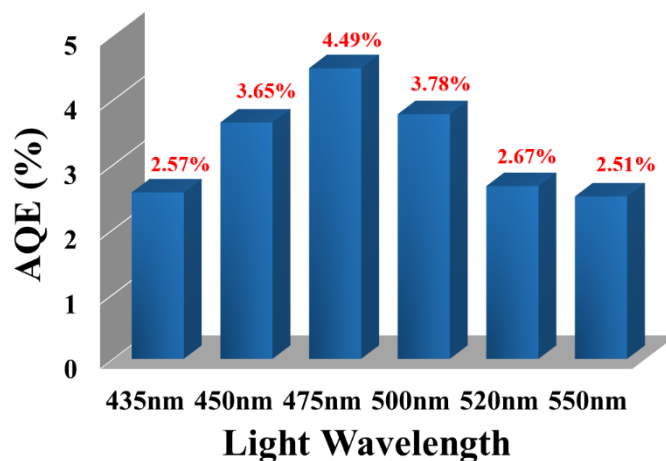


Figure S23. Apparent quantum efficiency values measured at six different wavelengths (435, 450, 475, 500, 520, 550 nm).

Table S2: Summary of H₂ Evolution Activity of COF-Based and CTF-Based Photocatalytic Systems.

Entry	Samples	Cocatalyst	HER		AQY	Ref.
			$\mu\text{mol g}^{-1} \text{h}^{-1}$	λ (nm)	[%]	
1	CdS:COF(90:10)	Pt	3678	420	4.2	6
2	TFPT-COF	Pt	1970	420	2.2	7
3	N ₃ -COF	Pt	1073	450	0.44	8
4	N ₂ -COF	Pt	438	450	0.19	8
5	N ₁ -COF	Pt	90	450	0.077	8
6	N ₀ -COF	Pt	23	450	0.001	8
7	N ₂ -COF	[Co(dmgh) ₂ pyCl]	782	400	0.16	9
8	CTF-10min	Pt	1072	450±10	9.2	10
9	PTP-COF	Pt	83.38	425-800	4.15	11
10	TP-BDDA	Pt	340±10	520	1.8	12
11	PTO-300>2.5	Pt	1076±278	400±20	5.5	13
12	Mo ₃ S ₁₃ @EB-COF	Ru(bpy) ₃ as photosensitizer	13215	475	4.49	This work

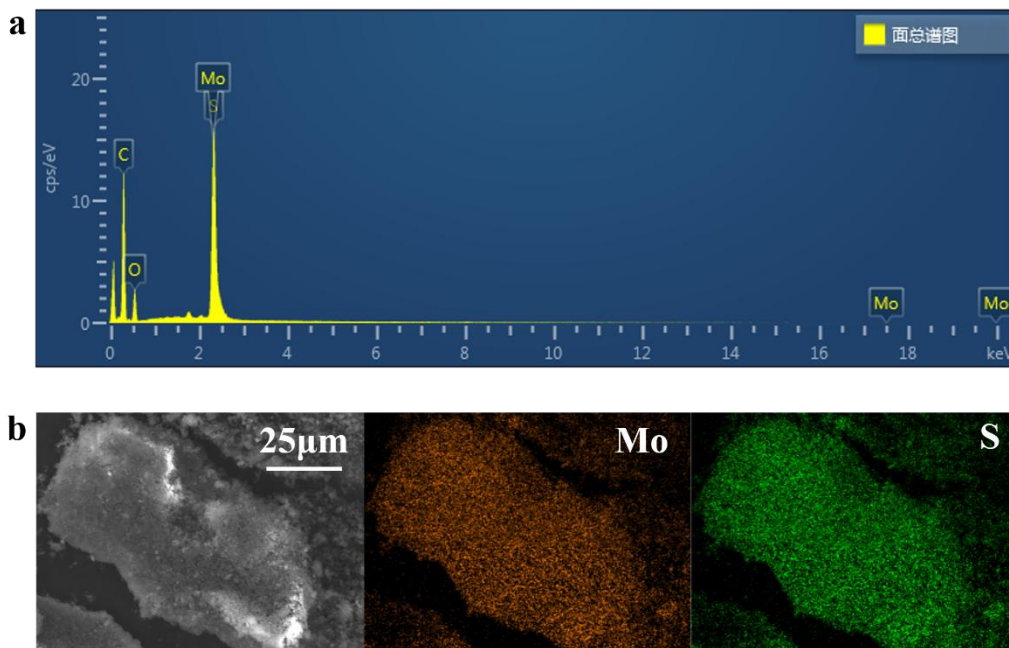


Figure S24. (a) EDS elemental analysis and (b) EDS elemental mapping of Mo_3S_{13} @EB-COF after four cycles.

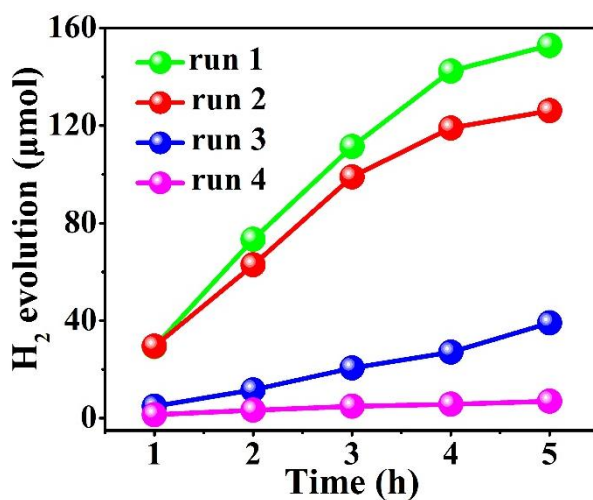


Figure S25. Cycle test of Mo_3S_{13} @EB-COF under visible light irradiation ($\lambda > 420\text{nm}$) for 4 times, 5 hours each time. Which was performed by recycling the reacted catalyst collected by centrifugation and washed several times, and adding fresh TEA and fluorescein.

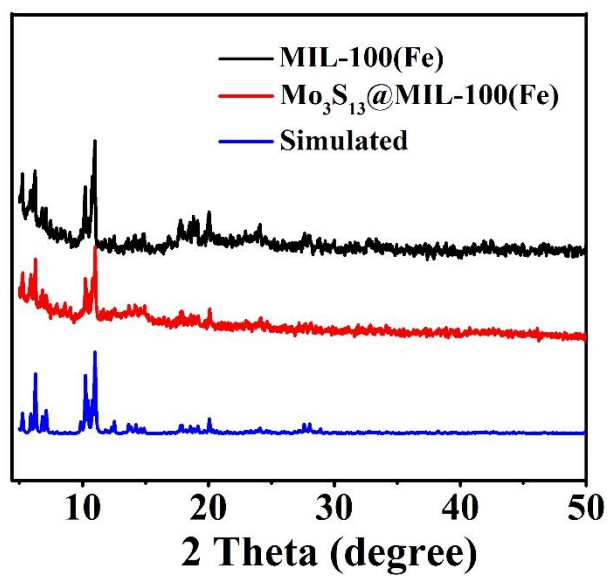


Figure S26. PXRD patterns of MIL-100(Fe) and Mo_3S_{13} @MIL-100(Fe).

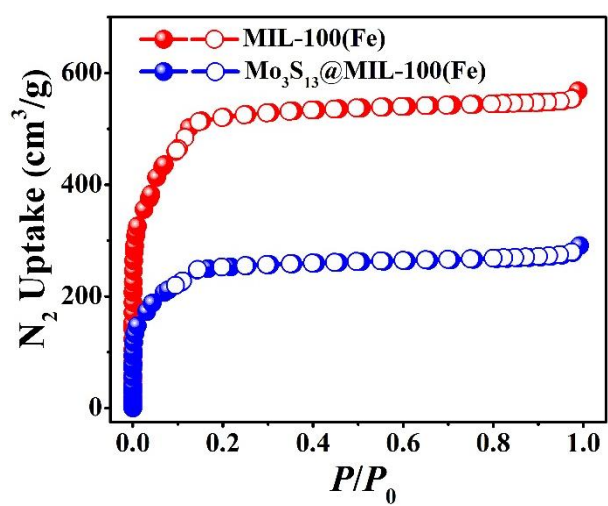


Figure S27. Nitrogen sorption isotherms for MIL-100(Fe) and Mo_3S_{13} @MIL-100(Fe).

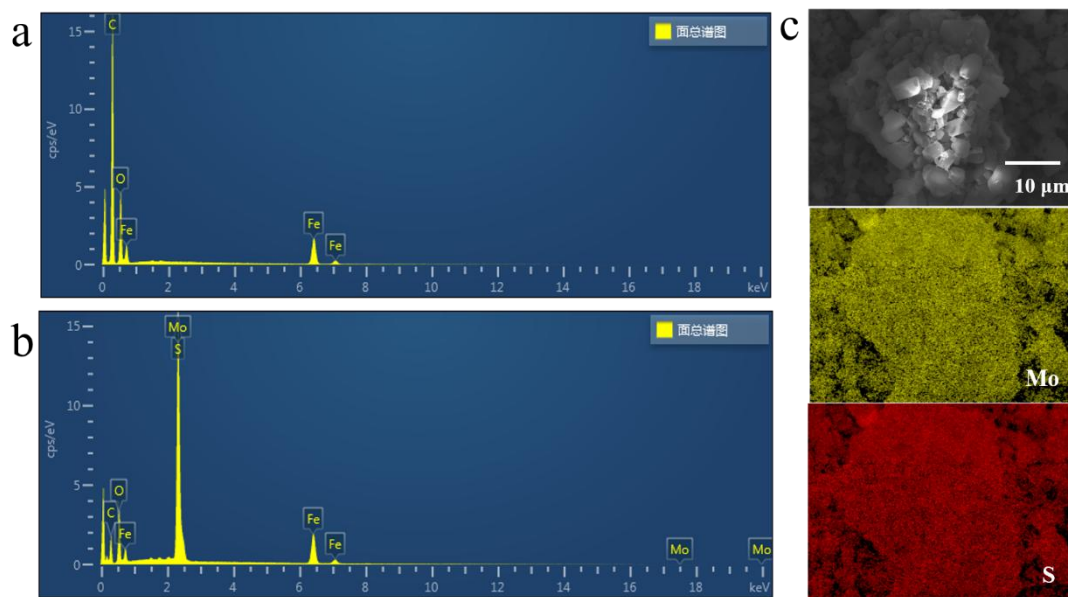


Figure S28. EDS elemental analysis of MIL-100(Fe) (a), Mo₃S₁₃@MIL-100(Fe) (b); The energy dispersive spectroscopy mapping of Mo₃S₁₃@MIL-100 (Fe) (c).

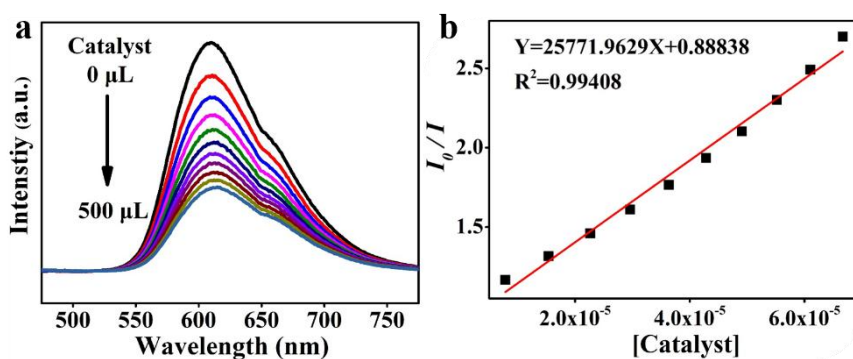


Figure S29. (a) Emission spectra of Ru(bpy)₃ as a function of Mo₃S₁₃@EB-COF. (b) Stern-Volmer plot for photoluminescence quenching of Ru(bpy)₃ by Mo₃S₁₃@EB-COF.

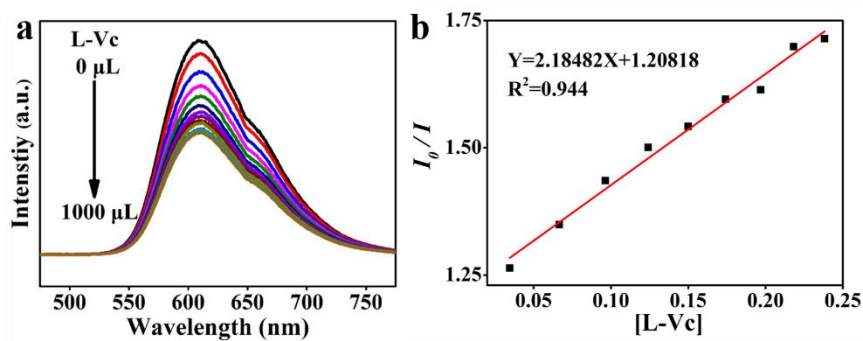


Figure S30. (a) Emission spectra of Ru(bpy)₃ as a function of L-Vc; (b) Stern-Volmer plot for photoluminescence quenching of Ru(bpy)₃ by L-Vc.

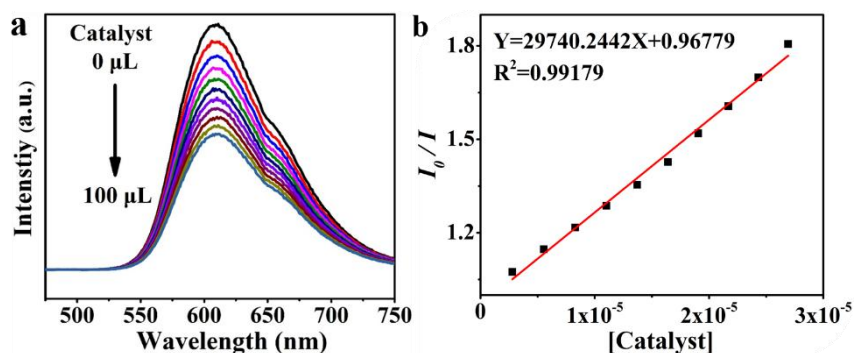


Figure S31. (a) Emission spectra of Ru(bpy)₃ as a function of MS-c; (b) Stern-Volmer plot for photoluminescence quenching of Ru(bpy)₃ by MS-c.

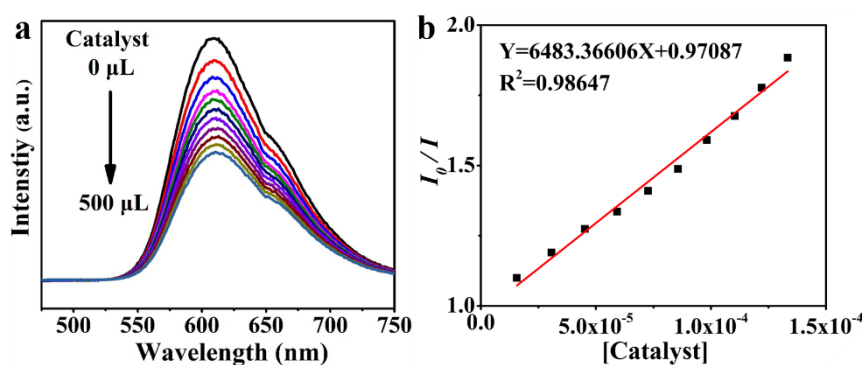


Figure S32. (a) Emission spectra of Ru(bpy)₃ as a function of Mo₃S₁₃@MIL-100(Fe); (b) Stern-Volmer plot for photoluminescence quenching of Ru(bpy)₃ by Mo₃S₁₃@MIL-100(Fe).

References

1. J. Tan, S. Namuangruk, W. F. Kong, N. Kungwan, J. Guo and C. C. Wang, *Angew. Chem. Int. Ed.*, 2016, **55**, 13979.
2. J. H. Chong, M. Sauer, B. O. Patrick and M. J. MacLachlan. *Org. Lett.*, 2003, **5**, 3823.
3. H. Ma, B. Liu, B. Li, L. Zhang, Y. Li, H. Tan, H. Zang and G. Zhu, *J. Am. Chem. Soc.*, 2016, **138**, 5897.
4. J. Kibsgaard, T. F. Jaramillo and F. Besenbacher, *Nat. Chem.*, 2014, **6**, 248.
5. P. Horcajada, S. Surblé, C. Serre, D. Y. Hong, Y. K. Seo, J. S. Chang, J. M. Grenèche, I. Margiolaki and G. Férey, *Chem. Commun.*, 2007, **27**, 2820.
6. J. Thote, H. B. Aiyappa, A. Deshpande, D. Díaz Díaz, S. Kurungot and R. Banerjee, *Chem. Eur. J.*, 2014, **20**, 15961.
7. L. Stegbauer, K. Schwinghammer and B. V. Lotsch, *Chem. Sci.*, 2014, **5**, 2789.
8. V. S. Vyas, F. Haase, L. Stegbauer, G. Savasci, F. Podjaski, C. Ochsenfeld and B. V. Lotsch, *Nat. Commun.*, 2015, **6**, 8508.
9. T. Banerjee, F. Haase, G. Savasci, K. Gottschling, C. Ochsenfeld and B. V. Lotsch, *J. Am. Chem. Soc.*, 2017, **139**, 16228.
10. S. Kuecken, A. Acharjya, L. J. Zhi, M. Schwarze, R. Schomäcker and A. Thomas, *Chem. Commun.*, 2017, **53**, 5854.
11. F. Haase, T. Banerjee, G. Savasci, C. Ochsenfeld and B. V. Lotsch, *Faraday Discuss.*, 2017, **201**, 247.
12. P. Pachfule, A. Acharjya, J. Roeser, T. Langenhahn, M. Schwarze, R. Schomäcker, A. Thomas and J. Schmidt, *J. Am. Chem. Soc.*, 2018, **140**, 1423.
13. K. Schwinghammer, S. Hug, M. B. Mesch, J. Senker and B. V. Lotsch, *Energy Environ. Sci.*, 2015, **8**, 3345.